

A new 3D beam formulation using full 3D constitutive laws

S. GAO^a, B. LIANG^a, E. VIDAL-SALLE^{a,b}

a. Université de Lyon, INSA-Lyon, LaMCoS UMR5259, F-69621, France

E-mail : sasa.gao@insa-lyon.fr; biao.liang@insa-lyon.fr

b. Corresponding author, E-mail: emmanuelle.vidal-salle@insa-lyon.fr

Abstract:

The present paper aims to present a new tool for modelling textile materials using the yarn as constitutive element. Modeling fabric process at the mesoscopic (i.e. the yarn) scale can be able to give realistic and physically fabric shape predictions. For that, the use of beam elements seems to be a good idea because fibre tows length is much higher than their transverse dimensions. Unfortunately, classical beam theories assume that the cross section acts as a rigid which can't describe the compression and shape change of the yarn. In this paper, we present a new 3D beam element with the aim to achieve the results with section changes while breaking from classical beam hypothesis. Inspired by previous works on the shell elements, we start from 2D beam element with thickness change by adding a normal strain component. Then, we extend the formulation to 3D beam elements by adding two coupling normal strain components so that full 3D constitutive strain-stress behaviour can be used directly. Finally, a FEM code is developed in Matlab and some numerical examples are presented using the new 3D beam elements which show that the results are exactly the same as those given by solid element in 3D element in ABAQUS/Standard.

Keywords:

Beam element; normal strain; full 3D constitutive laws; section deformation

1 Introduction

The need of efficient modelling of textile materials at meso-scale increased considerably in the last decade. Several approaches have been proposed which present different kinds of drawbacks, the most important being their high computation time. In order to save time (and money), it is of primary importance to reduce the time between the product idea and its delivery. To achieve this goal, it is necessary to have a good comprehension of the fabric behaviour. A large amount of studies have been developed to understand and model the fabric behaviour at micro- (fibre) or meso- (yarn) scale [1-7]. Those works have shown some mechanical analyses have been performed in which each fibre is considered as a 3D beam interacting with its numerous neighbours [3]. The very large number of fibres within a yarn results in large computation times. For computational reasons, those modelling are generally limited to a small piece of fabric so that the whole composite part is generally modelled at higher scale considering the textile preform as a continuum [8-11]. These macroscopic simulations

consider the deformation of a whole preform (in particular to simulate draping processes), then the internal woven structure of the fabric is not described. An intermediate way consists in developing models for yarns or tows, considered as continuous media, it is possible to build intermediate approaches to the behaviour of fabrics at a mesoscopic scale, considering the fabric as an assembly of interlacing tows (or yarns). Some approaches are available in the references concerning the modelling of fabrics at mesoscopic scale, considering the yarns as beams that bend according to the beam theory [12] or shell elements [13,14]. Using structural elements seems a good idea because of the geometry of the yarn, unfortunately, classical beam theories assume that the cross section acts as a rigid which can't describe the transverse deformation of the yarn (i.e. its compression and shape change), which is essential to the yarn behaviour.

The objective of the present paper is to propose a new 3D beam element with section changes which can be used to model yarn at the mesoscopic scale and describe its transverse behaviour. Inspired by previous works on enriched shell elements [15] where an additional node is introduced in the centre of three-node and four-node shell elements with two through-thickness translational degrees of freedom which makes it possible to extend plane stress state into full 3D elasticity. Using the same idea, a 2D beam element with thickness change is built by adding a central node with two degrees of freedom to an initially 2 nodes element. After the validation of that first development step, the formulation is extended into three-dimensional, which takes the deformation of cross section into account. Finally, a series of numerical examples are carried out, and the results are systematically compared with corresponding values of ABAQUS/Standard, which don't show any significant discrepancies.

2 2D beam elements with thickness change

Classical shell elements based on the degenerated shell concept or classical shell theories generally include the assumption of a plane stress state and can handle analyses of shells satisfactorily. However, problems may arise when they are used to simulate sheet metal forming because the normal stress in the thickness direction is omitted. In order to solve this problem, several authors [15,16] have proposed a new approach with an additional node which is introduced with two through-thickness translational degrees of freedom. Then full 3D constitutive strain-stress behaviour can be used. Such enrichment can be applied to other structural elements like beams.

Inspired by the methodology of shell elements described above, we build a 2D beam element with thickness change by introducing a central node to an initially 2 nodes element, as shown in Fig.1. The length is noted as L ($x_1 = -L/2, x_2 = 0, x_3 = L/2$), thickness is h . The centre node has two degrees of freedom corresponding to the relative displacements of the top and bottom surfaces of a beam respectively called v_2^+, v_2^- , which are dedicated to the normal strain so that we can calculate the thickness change. The relative displacements are defined as: $v_2^+ = v_2^t - v_2$, $v_2^- = v_2^b - v_2$, where v_2^t and v_2^b correspond to the normal displacement of top and bottom surfaces facing node 2 respectively, and $v_2 = (v_1 + v_3)/2$.

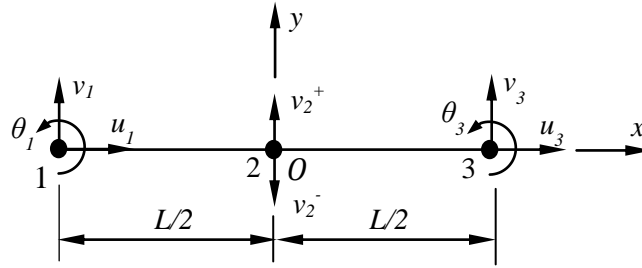


Fig.1 Additional of two degrees of freedom on Timoshenko beam element

In order to obtain linear distribution strain in thickness direction, the function $v(x, y)$ should be quadratic, so we assume a quadratic polynomial for $v(x, y)$.

$$v(x, y) = v(x, 0) + V_1(y)v_2^+ + V_2(y)v_2^- \quad (1)$$

Where, $V_1(y)$ and $V_2(y)$ are shape functions in thickness direction.

$$V_1(y) = \frac{y}{h} + \frac{2y^2}{h^2}, V_2(y) = -\frac{y}{h} + \frac{2y^2}{h^2} \quad (2)$$

Nodes 1 and 3 have 3 degrees of freedoms u_i, v_i, θ_i , as nodal variables, and the interpolation function within each element is dealt as Timoshenko beam. Due to the strain-displacement relation, we can get:

$$\begin{bmatrix} \varepsilon_{xx} \\ \varepsilon_{yy} \\ \gamma_{xy} \end{bmatrix} = \begin{bmatrix} H_1' & 0 & -yH_1' & 0 & 0 & H_3' & 0 & -yH_3' \\ 0 & 0 & 0 & V_1' & V_2' & 0 & 0 & 0 \\ 0 & H_1' & -H_1' & 0 & 0 & 0 & H_3' & -H_3' \end{bmatrix} \{d^e\} = [B] \{d^e\} \quad (3)$$

Where, $[B]$ is the element gradient matrix, and $\{d^e\}$ is the nodal displacement vector. $H_1(x)$ and $H_3(x)$ are shape function: $H_1(x) = 1/2(1 - \xi)$, $H_3(x) = 1/2(1 + \xi)$, $\xi = 2x/L$. For simplicity, notations, V_1, V_2, H_1 and H_3 will be used instead of $V_1(y), V_2(y), H_1(x)$ and $H_3(x)$; V_1', V_2', H_1' and H_3' as the derivative of $V_1(y), V_2(y), H_1(x)$ and $H_3(x)$.

Compared with Timoshenko beam, the shear strain remains unchanged except that the usual shear factor (whose value is normally 5/6 for a rectangular cross-section while 9/10 for a circular cross-section) is not used directly [15], and $2\varepsilon_{xy}$ becoming:

$$2\varepsilon_{xy} = g_y \gamma_{xy}, g_y = \frac{5}{4} \left(1 - 4 \frac{y^2}{h^2}\right) \quad (4)$$

As a result, the element gradient matrix $[B]$ becomes:

$$[B] = \begin{bmatrix} H_1' & 0 & -yH_1' & 0 & 0 & H_3' & 0 & -yH_3' \\ 0 & 0 & 0 & V_1' & V_2' & 0 & 0 & 0 \\ 0 & g_y H_1' & -g_y H_1' & 0 & 0 & 0 & g_y H_3' & -g_y H_3' \end{bmatrix} \quad (5)$$

The element stiffness matrix can be expressed as

$$[K^e] = \int_{\Omega_e} [B]^T [D] [B] d\Omega \quad (6)$$

in which Ω_e denotes the element domain, $[D]$ is the material property for the plane stress behaviour.

One thing to be noticed here, the shear strain energy should be under-integrated in order to prevent shear locking.

3 Extension to 3D beam element with section changes

In this section, a behaviour which remains elastic and isotropic is used but without the plane stress assumption and the goal is to extend it to full 3D elasticity. Compared with the 2D beam elements, the main novelty consists in the addition of extra degrees of freedoms on the central node, which can represent the thickness and wideness changes. In this way, the new 3D beam element formulation should include these main features as follows: each element has two end nodes which are treated by combining Saint-Venant and Timoshenko hypothesis; the normal strain of both thickness and wideness direction are introduced based on the additional central node. The formulation of displacement is completely quadratic by adding the terms coupling the deformation in both transverse directions; fully three-dimensional constitutive relation can be used directly. Under this theory, the proposed 3D beam element is firstly built with 2 end nodes with 6 degrees of freedom ($u_{xi}, u_{yi}, u_{zi}, \alpha_{xi}, \alpha_{yi}, \alpha_{zi}$), as described in the Fig.2, the element length is noted as L ($x_1 = -L/2, x_2 = 0, x_3 = L/2$), thickness is h and wideness is b . A central node with 8 degrees of freedom is added to describe the transverse deformation. Corresponding degrees of freedom are described in Fig.3, four relative translations in thickness direction namely $v_a^+, v_b^+, v_c^+, v_c^-$, and four in wideness direction namely $w_a^+, w_c^+, w_c^-, w_d^+$ respectively.

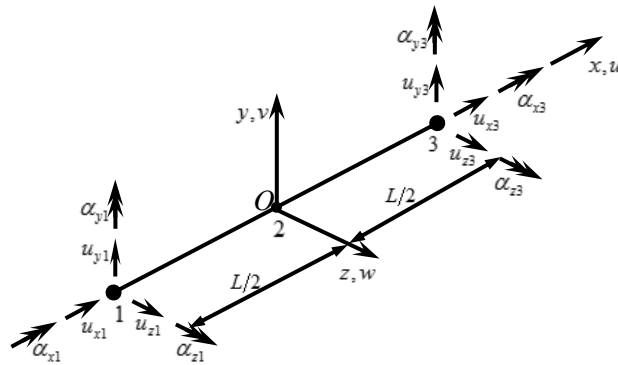


Fig.2 Additional of a central node based 3D Timoshenko beam

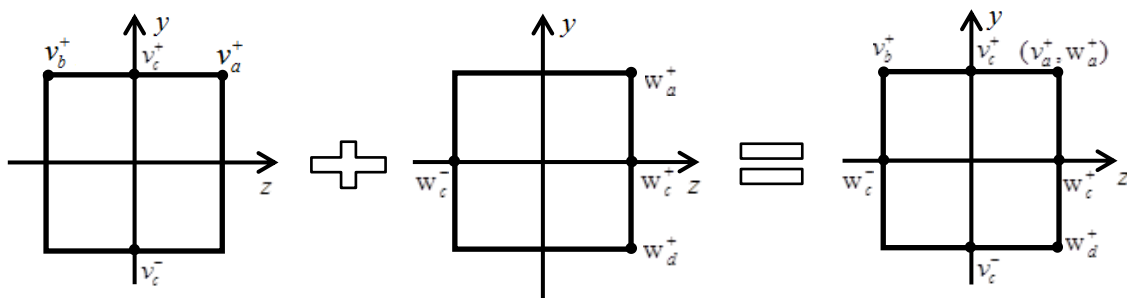


Fig.3 Presentation of the additional node with 8 degrees of freedom

Here, we define the relative displacements are defined as: $v_c^+ = v_c^t - v_2$, $v_c^- = v_c^b - v_2$, $v_a^+ = v_a^t - v_2$, $v_b^+ = v_b^t - v_2$. The superscript “t” represents the top surface, and the “b” represents the bottom surface. In order to make the deformation of cross section closer to the reality, we define the deformation function in thickness as:

$$v(x, y, z) = v(x, 0, 0) + V_1 v_c^+ + V_2 v_c^- + V_3 v_a^+ + V_4 v_b^+ \quad (7)$$

$$\text{Where, } V_1 = \frac{y}{h} + \frac{2y^2}{h^2} - \frac{4z^2}{b^2}, V_2 = -\frac{y}{h} + \frac{2y^2}{h^2}, V_3 = \frac{2yz}{bh} + \frac{2z^2}{b^2}, V_4 = -\frac{2yz}{bh} + \frac{2z^2}{b^2}.$$

Similarly, the deformation function in wideness direction can be expressed as:

$$w(x, y, z) = w(x, 0, 0) + W_1 w_c^+ + W_2 w_c^- + W_3 w_a^+ + W_4 w_d^+ \quad (8)$$

$$\text{Where, } W_1 = \frac{z}{b} + \frac{2z^2}{b^2} - \frac{4y^2}{h^2}, W_2 = -\frac{z}{b} + \frac{2z^2}{b^2}, W_3 = \frac{2yz}{bh} + \frac{2y^2}{h^2}, W_4 = -\frac{2yz}{bh} + \frac{2y^2}{h^2}.$$

For node 1 and node 3, we assume the simple linear shape function H_1 and H_3 (as described in section 2) for the variables $u_x, u_y, u_z, \alpha_x, \alpha_y, \alpha_z$. Due to the strain-displacement relation, the strains of the proposed 3D beam element can be expressed:

$$[\varepsilon] = [B] \{d^e\} \quad (9)$$

Where,

$$[B] = \begin{bmatrix} H_1' & 0 & 0 & 0 & zH_1' & -yH_1' & 0 & 0 & 0 & 0 & 0 & 0 & 0 & 0 & H_3' & 0 & 0 & 0 & zH_3' & -yH_3' \\ 0 & 0 & 0 & 0 & 0 & 0 & \frac{\partial V_1}{\partial y} & \frac{\partial V_2}{\partial y} & \frac{\partial V_3}{\partial y} & \frac{\partial V_4}{\partial y} & 0 & 0 & 0 & 0 & 0 & 0 & 0 & 0 & 0 & 0 \\ 0 & 0 & 0 & 0 & 0 & 0 & 0 & 0 & 0 & 0 & \frac{\partial W_1}{\partial z} & \frac{\partial W_2}{\partial z} & \frac{\partial W_3}{\partial z} & \frac{\partial W_4}{\partial z} & 0 & 0 & 0 & 0 & 0 & 0 \\ 0 & H_1' & 0 & -zH_1' & 0 & -H_1 & 0 & 0 & 0 & 0 & 0 & 0 & 0 & 0 & 0 & H_3' & 0 & -zH_3' & 0 & -H_3 \\ 0 & 0 & H_1' & yH_1' & H_1 & 0 & 0 & 0 & 0 & 0 & 0 & 0 & 0 & 0 & 0 & 0 & H_3' & yH_3' & H_3 & 0 \\ 0 & 0 & 0 & 0 & 0 & 0 & \frac{\partial V_1}{\partial z} & \frac{\partial V_2}{\partial z} & \frac{\partial V_3}{\partial z} & \frac{\partial V_4}{\partial z} & \frac{\partial W_1}{\partial y} & \frac{\partial W_2}{\partial y} & \frac{\partial W_3}{\partial y} & \frac{\partial W_4}{\partial y} & 0 & 0 & 0 & 0 & 0 & 0 \end{bmatrix}$$

$$[\varepsilon] = [\varepsilon_{xx} \quad \varepsilon_{yy} \quad \varepsilon_{zz} \quad \gamma_{yz} \quad \gamma_{xz} \quad \gamma_{xy}]^T$$

$$\{d^e\} = \{u_{x1} \quad u_{y1} \quad u_{z1} \quad \alpha_{x1} \quad \alpha_{y1} \quad \alpha_{z1} \quad v_c^+ \quad v_c^- \quad v_a^+ \quad v_b^+ \quad w_c^+ \quad w_c^- \quad w_a^+ \quad w_d^+ \quad u_{x3} \quad u_{y3} \quad u_{z3} \quad \alpha_{x3} \quad \alpha_{y3} \quad \alpha_{z3}\}^T$$

Same situation as the 2D beam element described previously the usual shear factor is not used directly, and $2\varepsilon_{xy}, 2\varepsilon_{xz}, 2\varepsilon_{yz}$ becoming:

$$\begin{aligned} 2\varepsilon_{xy} &= g_y \gamma_{xy}, 2\varepsilon_{xz} = g_z \gamma_{xz}, 2\varepsilon_{yz} = g_z \gamma_{yz} \\ g_y &= \frac{5}{4} \left(1 - 4 \frac{y^2}{h^2}\right), g_z = \frac{5}{4} \left(1 - 4 \frac{z^2}{b^2}\right) \end{aligned} \quad (10)$$

4 Numerical validation for linear small strain conditions

In this section, a series of examples are used to prove that the results obtained with the proposed 3D elements are nearly similar to those given by the solid elements from ABAQUS/Standard. In these examples, we consider a cantilever beam with length $l=10mm$, width $b=1mm$ and thickness $h=1mm$. Material parameters are: Young's modulus $E = 2.1 \times 10^5 MPa$, and Poisson's ratio $\nu = 0.3$. The cantilever beam is subjected to the action of axial force P, shear force F, and compression Q, respectively. A FEM code has been developed in Matlab, and a mesh of 10 elements for cantilever is used for calculations as shown in Fig.4(a). Then the results are compared with corresponding results from 3D ABAQUS/Standard simulations which have at least 640 elements (C3D8I) for calculating the same example shown in Fig.4 (b).

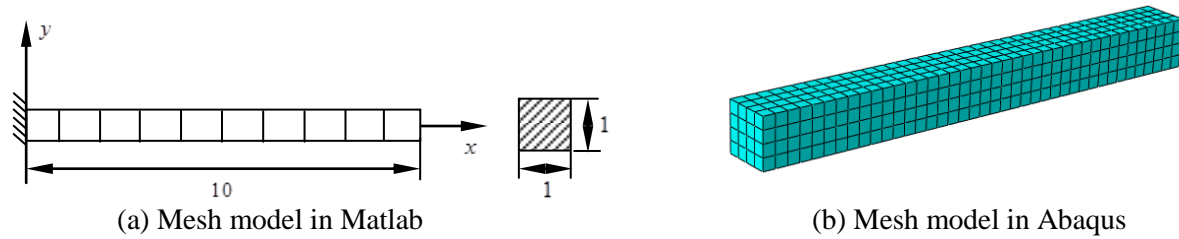
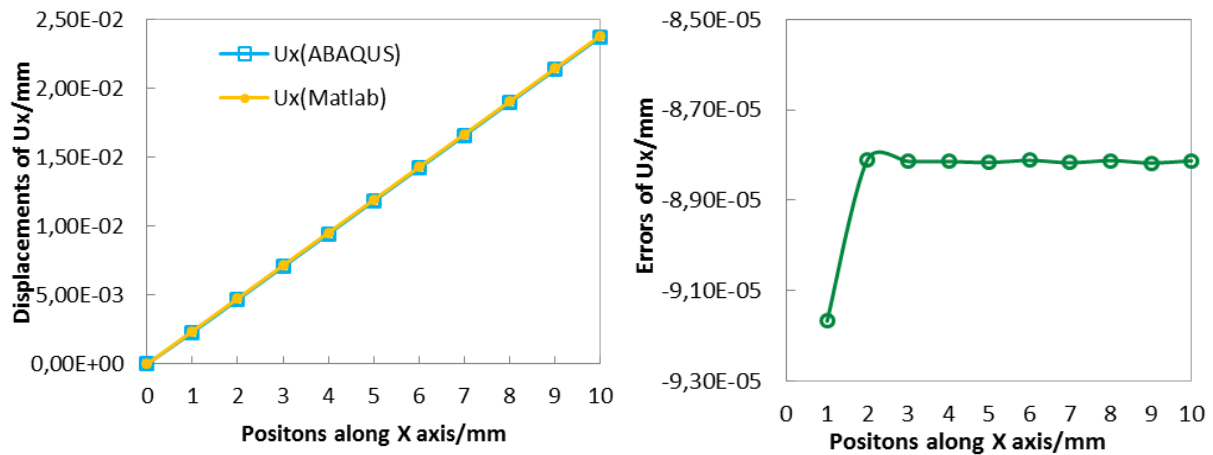


Fig.4 Mesh model

4.1 Tension

In this example, a cantilever beam is subjected to an axial load of 500N at the right end. The results given by the proposed 3D beam element in Matlab and solid element in ABAQUS/Standard can be seen in Fig.5(a), where, U_x represents the axial displacement. Here, we define the difference between the two results as errors to express the results more intuitively, $U_{xError} = U_{xAbaqus} - U_{xMatlab}$, as shown in Fig.5(b). From the figure, we can see that all the errors are at 10^{-5} mm orders of magnitude which remain stable except the value at the boundary. In such loading case, the transverse displacements present too symmetries with respect to the principal axis of the cross section: $v_c^+ = -v_c^-$, $v_a^+ = v_b^+$, $w_c^+ = -w_c^-$, $w_a^+ = w_d^+$, so it is not necessary to observe the 8 calculated displacements. Only 4 values are sufficient. Table.1 presents those values from both ABAQUS and Matlab simulations. The results presented the identical so that one can conclude that the proposed approach is able to describe the section behaviour under tensile loading.



(a) Displacement distribution of U_x (b) Distribution of displacement errors U_{xError}

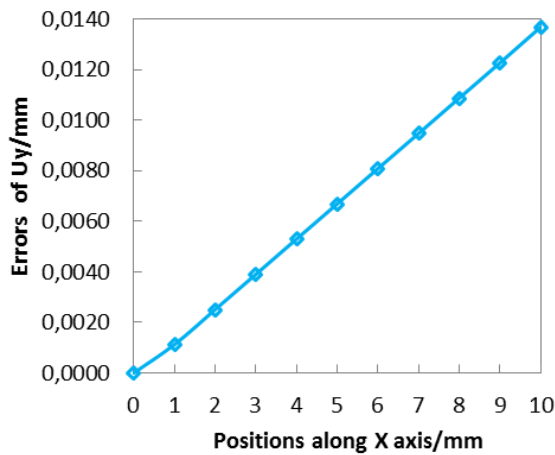
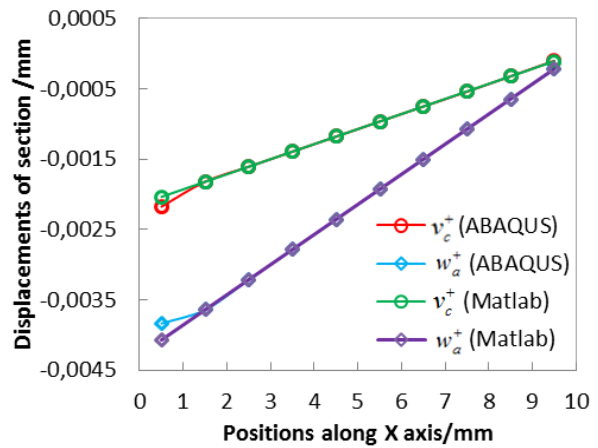
Fig.5 The results comparison of ABAQUS and Matlab under tension

Table.1 Cross section deformation comparison of ABAQUS and Matlab under tension

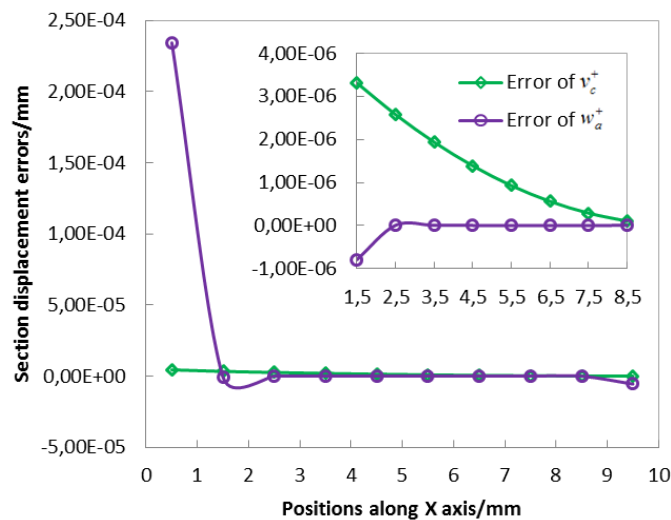
	v_c^+	v_a^+	w_c^+	w_a^+
ABAQUS	-0,00035714	-0,00035714	0,00035714	0,00035714
MATLAB	-0,00035714	-0,00035714	0,00035714	0,00035714

4.2 Shear + bending

In this example, we discuss the cantilever beam subjected to a concentrated force $F=-100\text{N}$ at the right end. The concentrated force not only has the effect of bending but also has the effect of shear. The comparisons between ABAQUS and Matlab results are shown in Fig.6. The errors of U_y ($U_{yError}=U_{yAbaqus}-U_{yMatlab}$) for the centroidal axis between the two results can be seen in Fig.6(a). The errors distribution is linear and the biggest value lies at the end of the cantilever beam, which is 0.0137mm . Compared with the biggest displacement at the end of the cantilever 1.915mm , the relative error is 0.7% . By solving the calculation model, we can obtain the conclusions such as: $v_c^+ = v_c^-, v_a^+ = v_b^+ = 0, w_c^+ = -w_c^- = 0, w_a^+ = -w_a^-$. Thus, we just need to compare the value of v_c^+ and w_a^+ , which can be seen in Fig.6(b). And the errors (defined the same way as the errors of U_y) correspond to v_c^+ and w_a^+ are expressed in Fig.6(c), all the values are nearly zero (10^{-7}mm orders of magnitude) except for those near the boundary, which proves the proposed 3D beam element can be used to simulate the beam under concentrated force and could obtain good results.

(a) Errors of U_y for the centroidal axis

(b) Relative displacement of cross section



(c) Displacement errors of cross section

Fig.6 The results comparison of ABAQUS and Matlab

4.3 Compression

Here, we consider a cantilever beam subjected to a uniformly distributed load $Q=50\text{N/mm}$ to demonstrate the ability of 3D beam element to simulate the section deformation occurring under the action of compression. The calculation model in Matlab is shown as Fig.7.

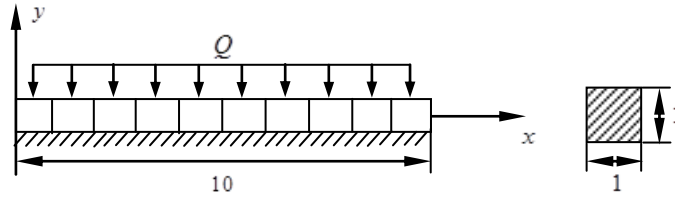


Fig.7 Cantilever under compression

For the proposed 3D beam element, we set the boundary as described in Fig.7, actually only the middle line is fixed. For simulation in ABAQUS, in order to set the same boundary conditions, we take 1/4 of beam model and set the symmetric boundary conditions. Under the action of compression, there is: $v_c^+ = -v_c^-$, $v_a^+ = v_a^-$, $w_c^+ = -w_c^-$, $w_a^+ = w_a^-$, and the values of v_c^+ , v_a^+ , w_c^+ , w_a^+ are constant along the positions of X axis, the results are listed in Table.2. From the comparison, it can be seen that we can use the proposed 3D beam elements to obtain the same results given by solid elements in ABAQUS.

Table.2 Cross section deformation comparison of ABAQUS and Matlab under compression

	v_c^+	v_a^+	w_c^+	w_a^+
ABAQUS	-0,00011905	-0,00011905	0,00003571	0,00003571
MATLAB	-0,00011905	-0,00011905	0,00003571	0,00003571

Such results show, if needed, that the 8 extra degrees of freedom are sufficient to introduce the coupling between ε_{yy} and ε_{zz} .

5 Conclusions and future developments

In this paper, a new 3D beam element with section changes has been proposed. It results from the evolution of an enriched shell element that has been firstly introduced in a 2D beam element in order to validate the interest of such technique. The new beam element is an evolution of a 2 nodes Timoshenko beam element with an extra node at mid-length. That extra node allows the introduction of 3 extra strain components: ε_{yy} , ε_{zz} and $2\varepsilon_{yz}$ so that a full 3D constitutive strain-stress behaviour can be used. For that, 8 degrees of freedom are required. The proposed element has been introduced in a Matlab finite element code and a series of validation cases have been treated and compared with 3D ABAQUS/Standard simulations. The results obtained are in good agreement and encouraging. The results presented in that paper are only the first step of a more ambitious work. Indeed, the final goal is to use those elements to model yarns in a textile composite preform. For that purpose, the two following steps are: (1) introducing anisotropic behaviour; (2) realising validation for large displacements and strains.

Acknowledgements

The authors would like to thank China Scholarship Council (CSC).

The authors also want to thank gorgeously Dr Francis Sabourin for his help and advices.

References

- [1] Q. T. Nguyen, E. Vidal-Sallé, P. Boisse, C. H. Park, A. Saouab, J. Bréard, G. Hivet, Mesoscopic scale analyses of textile composite reinforcement compaction, *Composites Part B: Engineering*. 44(2) (2013) 231-241.
- [2] P. Badel, E. Vidal-Sallé, P. Boisse, Computational determination of in-plane shear mechanical behaviour of textile composite reinforcements, *Computational materials science*. 40(4)(2007) 439-448.
- [3] G. Zhou, X. Sun, Y. Wang, Multi-chain digital element analysis in textile mechanics, *Composites science and Technology*. 64(2) (2004) 239-244.
- [4] D. Durville, Simulation of the mechanical behaviour of woven fabrics at the scale of fibers, *International journal of material forming*. 3(2) (2010) 1241-1251.
- [5] A. Charmetant, E. Vidal-Sallé, P. Boisse, Hyperelastic modelling for mesoscopic analyses of composite reinforcements, *Composites Science and Technology*. 71(14) (2011) 1623-1631.
- [6] P. Latil, L. Orgéas, C. Geindreau, P.J. J. Dumont, S. Rolland du Roscoat, Towards the 3D in situ characterisation of deformation micro-mechanisms within a compressed bundle of fibres, *Composites Science and Technology*. 71(4) (2011)480-488.
- [7] P. Badel, E. Vidal-Sallé, E. Maire, P. Boisse, Simulation and tomography analysis of textile composite reinforcement deformation at the mesoscopic scale, *Composites Science and Technology*. 68(12) (2008)2433-2440.
- [8] M. J. King, P. Jearanaisilawong, S. Socrate, A continuum constitutive model for the mechanical behavior of woven fabrics, *International Journal of Solids and Structures*. 42(13)(2005)3867-3896.
- [9] X.Q. Peng, J. Cao, A continuum mechanics-based non-orthogonal constitutive model for woven composite fabrics, *Composites part A: Applied Science and manufacturing*. 36(6) (2005) 859-874.
- [10] B.Liang, N. Hamila, M. Peillon, P. Boisse, Analysis of thermoplastic prepreg bending stiffness during manufacturing and of its influence on wrinkling simulations, *Composites Part A: Applied Science and Manufacturing*. 67(2014)111-122.
- [11] M.A. Khan, T. Mabrouki, E. Vidal-Sallé, P. Boisse, Numerical and experimental analyses of woven composite reinforcement forming using a hypoelastic behaviour. Application to the double dome benchmark, *Journal of Materials Processing Technology*. 210(2) (2010)378-388.
- [12] C. Lekakou, M.A.K. BJohari, M.G. Bader, Compressibility and flow permeability of two-dimensional woven reinforcements in the processing of composites, *Polymer Composites*. 17(5) (1996) 666-672.
- [13] S. Gatouillat, E. Vidal-Sallé, P. Boisse, Advantages of the meso/macro approach for the simulation of fibre composite reinforcements, *International Journal of Material Forming*. 3(1) (2010) 643-646.
- [14] S. Gatouillat, E. Vidal-Sallé, P. Boisse, Approche mésoscopique pour la mise en forme des renforts tissés de composites, *Comptes-rendus des 17èmes Journées Nationales sur les Composites (JNC17)*. 2014.
- [15] M. Sansalone, F. Sabourin, M. Brunet, A new shell formulation using complete 3D constitutive laws, *International Journal for Numerical Methods in Engineering*. 86(6) (2011).688-716.
- [16] B. Bassa, F. Sabourin, M. Brunet, A new nine-node solid-shell finite element using complete 3D constitutive laws, *International Journal for Numerical Methods in Engineering*. 92(7) (2012)589-636.